Title

Targeting nuclear receptor corepressors for reversible male contraception.

Journal

Proceedings of the National Academy of Sciences, 121(9)

Authors

Hong, Suk-Hyun

Castro, Glenda

Wang, Dan

et al.

Publication Date

2024-02-27

DOI

10.1073/pnas.2320129121

Peer reviewed

PNAS RESEARCH ARTICLE | PHYSIOLOGY

Targeting nuclear receptor corepressors for reversible male contraception

Suk-Hyun Hong[a], Glenda Castro[a], Dan Wang[a,1], Russell Nofsinger[a], Maureen Kane[b], Alexandra Folias[b], Annette R. Atkins[a], Ruth T. Yu[a], Joseph L. Napoli[b], Paolo Sassone-Corsi[c], Dirk G. de Rooij[d], Christopher Liddle[e], Michael Downes[a], and Ronald M. Evans[a,2]

Contributed by Ronald M. Evans; received November 30, 2023; accepted January 6, 2024; reviewed by Yanhong Shi and Henry M. Sucov

Despite numerous female contraceptive options, nearly half of all pregnancies are unintended. Family planning choices for men are currently limited to unreliable condoms and invasive vasectomies with questionable reversibility. Here, we report the development of an oral contraceptive approach based on transcriptional disruption of cyclical gene expression patterns during spermatogenesis. Spermatogenesis involves a continuous series of self-renewal and differentiation programs of spermatogonial stem cells (SSCs) that is regulated by retinoic acid (RA)–dependent activation of receptors (RARs), which control target gene expression through association with corepressor proteins. We have found that the interaction between RAR and the corepressor silencing mediator of retinoid and thyroid hormone receptors (SMRT) is essential for spermatogenesis. In a genetically engineered mouse model that negates SMRT-RAR binding (SMRT^{mRID} mice), the synchronized, cyclic expression of RAR-dependent genes along the seminiferous tubules is disrupted. Notably, the presence of an RA-resistant SSC population that survives RAR de-repression suggests that the infertility attributed to the loss of SMRT-mediated repression is reversible. Supporting this notion, we show that inhibiting the action of the SMRT complex with chronic, low-dose oral administration of a histone deacetylase inhibitor reversibly blocks spermatogenesis and fertility without affecting libido. This demonstration validates pharmacologic targeting of the SMRT repressor complex for non-hormonal male contraception.

spermatogenesis | retinoic acid signaling | transcriptional corepression

Significance

With unintended pregnancies costing billions of dollars a year in the United States alone, the socioeconomic and health benefits of improved birth control cannot be overemphasized. Despite the pressing need for population control, male contraceptive options are limited. These rodent studies demonstrate reversible male contraception by targeting silencing mediator of retinoid and thyroid hormone receptors-retinoid acid receptor signaling to identify a non-hormonal approach to male contraception.

With unintended pregnancies costing billions of dollars a year in the United States alone, the socioeconomic and health benefits of improved birth control cannot be overemphasized (1). Despite the pressing need for population control, male contraceptive options are limited. The contraceptive choices for men are restricted to condoms with high failure rates and invasive, potentially irreversible vasectomies. New approaches to male contraception such as directly blocking spermatogenesis, preventing sperm maturation, or inhibiting fertilization have had only limited success, providing either incomplete protection or severe side effects (1). The lack of effective male contraceptive options may be due to the complex nature of spermatogenesis, a retinoic acid receptor (RAR)-regulated series of self-renewal and differentiation programs of spermatogonial stem cells (SSCs) in testicular somatic niche cells. Pharmacological inhibition of retinoic acid (RA) production (2–4) or RAR antagonism (5–7) in the testes to transiently block SSC differentiation and spermatogenesis has been explored as a potential strategy, but the progress is incremental. Therefore, an alternative approach is needed to identify and validate candidate contraceptives that can control testicular RA signaling to halt spermatogenesis without permanently damaging the reproductive system while retaining the SSC population. Identifying additional players controlling this complex system has been challenging.

The roles of the RA ligand and its RAR receptors are critical in spermatogenesis (8). In the absence of cognate ligands, RARs are bound by corepressors such as silencing mediator of retinoid and thyroid hormone receptors (SMRT). In the un-liganded state, RAR forms a transcriptionally repressive complex with SMRT and histone deacetylases (HDACs), the RAR–SMRT–HDAC complex, that limits chromatin access to the transcriptional machinery. Upon ligand binding, this repressive complex dissociates. The subsequent recruitment of coactivator complexes facilitates dose-dependent transcription, such that RAR functions as a transcriptional rheostat rather than a binary "on–off" switch. RARs have been studied extensively in the context of spermatogenesis, where genetic deletion of RAR (9), or depletion of its agonist precursor Vitamin A results in the arrest of both SSC differentiation and spermatogenesis (10, 11). With a critical role in SSC self-renewal and differentiation, RA production and degradation are tightly regulated in the seminiferous tubules (12, 13). Seminiferous tubules are shielded from the systemic level of

Author affiliations: [a]Gene Expression Laboratory, Salk Institute for Biological Studies, La Jolla, CA 92037; [b]Department of Nutritional Sciences and Toxicology, The University of California, Berkeley, CA 94720; [c]Department of Biological Chemistry, Center for Epigenetics and Metabolism, U1233 INSERM, University of California, Irvine, CA 92697; [d]Reproductive Biology Group, Division of Developmental Biology, Department of Biology, Faculty of Science, Utrecht University, 3584 CH Utrecht, The Netherlands; and [e]Storr Liver Centre, The Westmead Institute for Medical Research and Sydney Medical School, University of Sydney, Westmead, NSW 2145, Australia

Author contributions: S.H.-H., J.L.N., P.S.-C., M.D., and R.M.E. designed research; S.H.-H., G.C., D.W., R.N., M.K., and A.F. performed research; S.H.-H., M.K., R.T.Y., and C.L. analyzed data; and S.H.-H., A.R.A., R.T.Y., D.G.d.R., C.L., M.D., and R.M.E. wrote the paper.

Reviewers: Y.S., Beckman Research Institute of City of Hope; and H.M.S., Medical University of South Carolina.

Competing interest statement: The authors disclose that the reviewer Y.S. jointly authored a commentary on an unrelated topic with RME in 2022 (PMID: 35344400).

[1]Present address: Oncogenesis Thematic Research Center—Translational Research, Bristol Myers Squibb, San Diego, CA 92121.

[2]To whom correspondence may be addressed. Email: evans@salk.edu.

This article contains supporting information online at https://www.pnas.org/lookup/suppl/doi:10.1073/pnas.2320129121/-/DCSupplemental.

Published February 20, 2024.

retinoids as peritubular myoid cells express Cyp26 enzymes in the outer basal lamina, in addition to tight, adherent and gap junctions of blood-testis barriers. Genetic deletion of RA-producing enzymes in mice phenocopies the compound deletion of Sertoli-RARα/Germ-RARγ in Sertoli cells and SSC-only testis, indicating that RA production is a key regulator of RAR action (14). Genetic deletion of the RA-degradation enzyme, Cyp26b1 in Sertoli/Germ cells in mice resulted in subfertility (15), emphasizing that the precise levels of RA and resulting RAR activation/repression are essential for normal spermatogenesis.

Here, we report that disabling the NR binding function of SMRT and thereby its interaction with RAR (SMRT^{mRID}) (16–18) in mice results in progressive testicular degeneration with the loss of stage-specific, cyclic gene expression. Moreover, exploiting the identification of a subset of SSCs resistant to the effects of RAR activation, we show that pharmacological modulation of the RAR-SMRT-HDAC complex functions as a non-hormonal, reversible contraceptive. These data implicate SMRT as an integral regulator of RAR signaling, whereby the RAR-SMRT-HDAC complex controls chromatin accessibility at key gene regulatory elements that govern spermatogenic programs in both germ SSCs and somatic Sertoli cells.

Results

Primary Spermatogenic Failure in SMRT^{mRID} Mice. Male homozygous SMRT^{mRID} mutant mice are sterile with progressive testicular degeneration evident around 1 mo of age compared to heterozygous control males (Fig. 1 *A*–*C*). While no differences were seen in the circulating levels of testosterone and Leydig cell-responsive luteinizing hormone (LH), Sertoli cell-responsive follicle-stimulating hormone (FSH) was elevated, suggesting primary spermatogenic failure in SMRT^{mRID} mice (Fig. 1*D*). These results are supported by the normal size of the seminal vesicles (SVs) as their growth is directly correlated with circulating testosterone levels (Fig. 1 *C* and *D*). Sexually mature SMRT^{mRID} mice display normal mounting behavior but there was virtually no mature sperm found in the caput epididymis (Fig. 1*E*). Spermatogenesis in the seminiferous tubules involves a progressive series of synchronized gametogenic sequences, known as the seminiferous epithelium cycle that is coordinately regulated by germ cells and supporting somatic cells including Sertoli cells. Of the twelve epithelium cycle stages in mouse spermatogenesis, SMRT^{mRID} seminiferous tubules show an incomplete block in differentiation of round spermatids at stage VIII (Fig. 1*F*). This stage occurs immediately before the RA-dependent spermiation step (Fig. 1*C*), implicating the interaction of SMRT with RAR as critical for this development (from step 8 round spermatids to spermiation takes one epithelial cycle = 8.6 d). The absence of mature sperm further supports a block in differentiation at the round spermatid stage. By 5 mo of age, many seminiferous tubules contain few germ cells in SMRT^{mRID} animals (Fig. 1*F*).

Vitamin A-Independent Spermatogenesis in SMRT^{mRID} Mice. SMRT is ubiquitously expressed throughout the testicular cell population, with the highest expression in Sertoli cells and subsets of germ cell nuclei (Fig. 1*G* and See *SI Appendix,* Fig. S1*A*). To investigate de-repressed RAR signaling in SMRT^{mRID} testes, we maintained newborn SMRT^{mRID} and control mice on a VAD diet for 7 mo to arrest differentiation of type A spermatogonia (19). Vitamin A deficiency was confirmed by the marked increase in SV size (Fig. 1*K* compared to Fig. 1*D*), as well as decreased liver retinol levels (*SI Appendix,* Figs. S1 *B* and *C*) in both control and SMRT^{mRID} mice. As expected, a complete block of spermatogenesis and arrested spermatogonia was evident in the tubules of control testes (Fig. 1*J*). In contrast, spermatogenesis was not arrested at the spermatogonial stage by vitamin A deficiency in SMRT^{mRID} mice, with mice displaying virtually identical patterns of spermatogenesis to those on a normal diet, emphasizing the importance of transcriptional repression by the SMRT-RAR complex. Nonetheless, defects and stage VIII block of spermatogenesis were evident in SMRT^{mRID} tubules, including inefficient spermiation and a depletion of differentiating germ cells. The loss of arrest at type A spermatogonia in SMRT^{mRID} mice suggests that corepressor-mediated repression is critical to control SSC differentiation. Indeed, the gradual loss of germ cells in SMRT^{mRID} mice may be the result of uncontrolled SSC differentiation, as the balance between self-renewal and differentiation is critical for sustainable spermatogenesis. Notably, a morphologically distinct RA-resistant PLZF+ SSC subpopulation was detected in 4-mo-old SMRT^{mRID} tubules (Fig. 1 *H* and *I*).

We next explored whether an RARα antagonist, delivered by osmotic pump into the tunica albuginea of the testes, could rescue defective spermatogenesis in SMRT^{mRID} mice (*SI Appendix,* Fig. S1*D*). On the contrary, 1 mo of RARα antagonist exposure further compromised spermatogenesis (*SI Appendix,* Fig. S1*E*). In comparison to vehicle-treated SMRT^{mRID} testes, many tubules show Sertoli-only phenotypes suggesting depletion of germ cells. The failure of an RAR antagonist treatment to rescue the infertility phenotype indicates that precise timing of RAR activation/repression is required during spermatogenesis.

Derepression of RAR in SMRT^{mRID} Germ Stem (GS) Cells. To gain mechanistic insight, the transcriptional changes induced by the RAR ligand, all trans-RA (ATRA) in both control and SMRT^{mRID} GS cells were determined with genome-wide transcriptome analysis. Clustering analysis identified four groups: Group I includes RA-inducible genes with similar expression levels across genotypes, and groups II and III include genes that are repressed in the absence of RA in SMRT^{mRID} cells (Fig. 2*A*). While the genes in group II were derepressed to control levels upon treatment with RA, those in group III were induced to levels above that of control cells upon RA treatment. Group IV includes RA-inducible genes that were de-repressed in SMRT^{mRID} cells including classic RAR target genes *Stra8*, *Sall4*, and *Rarb* (Fig. 2*A*). Gene ontology (GO) analyses revealed that the genes in group IV are involved in meiotic recombination and RAR signaling. Additionally, RA catabolism genes such as *Cyp26a1* were found in group IV, raising the possibility that enhanced RA clearance allows SSCs to evade RA-mediated differentiation signals to ensure their survival in SMRT^{mRID} de-repression.

Profound Asynchrony of Spermatogenic Progression in SMRT^{mRID} Mice. In isolated Sertoli cells, pathway analysis of the differentially expressed genes between CTRL and SMRT^{mRID} mice revealed a significant upregulation of apoptotic, focal adhesion, and regulation of actin cytoskeleton pathways (Fig. 2*B* and *SI Appendix,* Fig. S2 *A* and *B*). Furthermore, ex vivo agonist and antagonist treatments of isolated Sertoli cells revealed disrupted RAR signaling in SMRT^{mRID}-derived cells (Fig. 2*C*).

The development of elongated spermatids from round spermatids requires the temporally and spatially synchronized replacement of histones with spermatid-specific protamines. This concerted replacement was disrupted in mutant testes, even during the prepubertal first round of spermatogenesis, with mixed stages of histone replacement evident in single seminiferous epithelium cycle stages (20, 21) (Fig. 2*D*). Transition proteins and protamines are

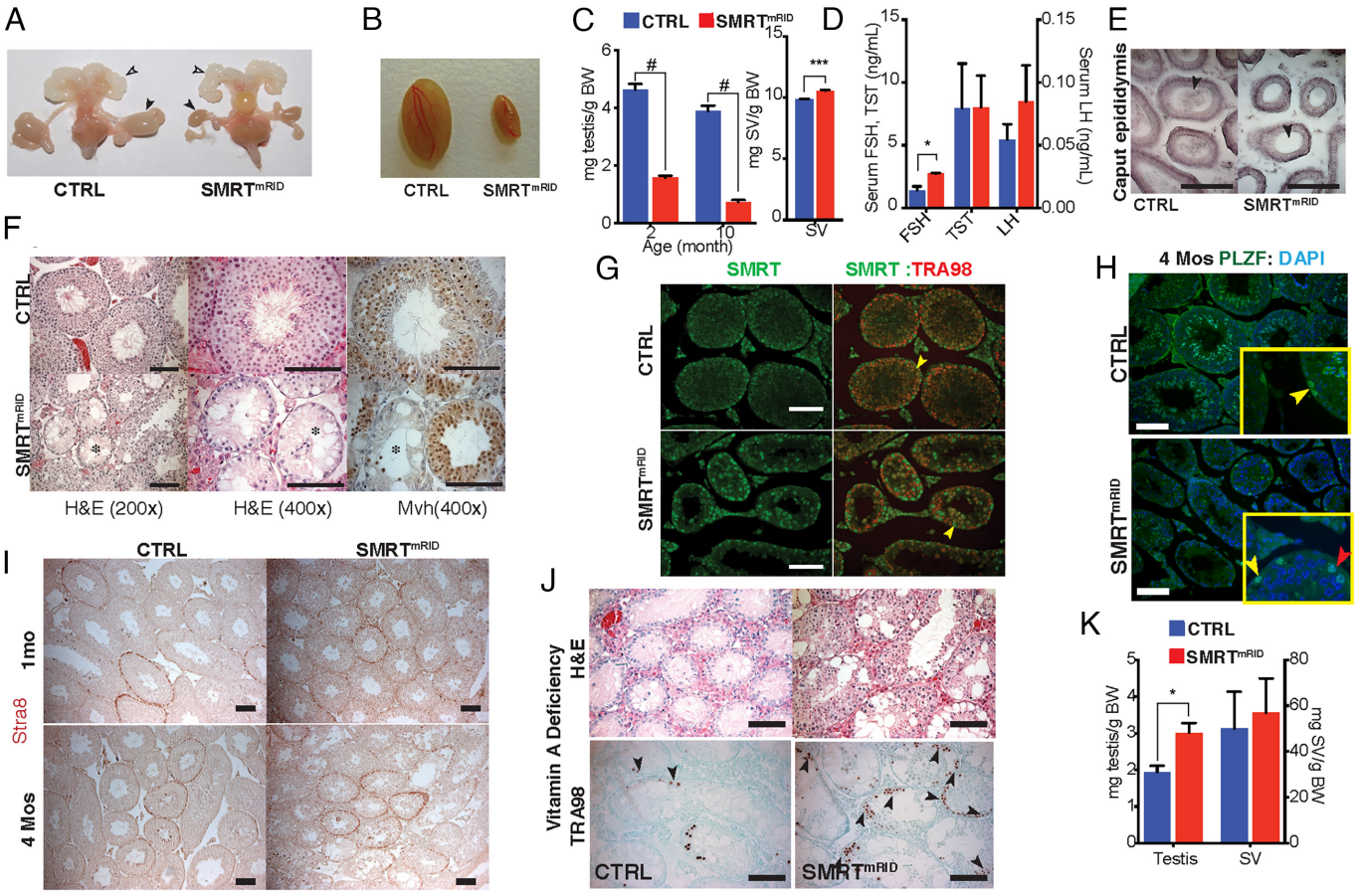

Fig. 1. Testicular degeneration and Vitamin A-independent spermatogenesis in SMRT^{mRID} mice. (*A*) Representative images of the urogenital system including SV (white arrowhead) and testes (black arrowhead) from control (CTRL) and SMRT^{mRID} mice at 5 mo. (*B*) Representative images of isolated testis from 10-mo-old CTRL and SMRT^{mRID} mice. (*C*) Normalized testis and SV weights (n = 12 for 2-mo-old, n = 9 for 10-mo-old, $^{\#\#}P < 5 \times 10^{-11}$; $^{***}P < 0.0005$). (*D*) Serum levels of FSH, testosterone (TST), and LH in CTRL and SMRT^{mRID} mice (n = 10, $^{*}P < 0.05$). (*E*) Mature sperm (black arrowhead) in CTRL but not SMRT^{mRID} caput epididymis. (*F*) Cross section of seminiferous tubules showing loss of germ cells (germ-cell-specific Mvh staining) and arrest at round spermatid stage in SMRT^{mRID} mice. * indicate tubule with significant germ cell depletion. (*G*) SMRT expression in seminiferous epithelium showing high expression in Sertoli nuclei. TRA98 is only expressed in germ cells. Yellow arrowheads indicate typical Sertoli cell nuclei. (*H*) PLZF^{+} spermatogonial stem cells (SSCs indicated by arrowheads) in testes from 4-mo-old CTRL and SMRT^{mRID} mice. (*I*) Stra8-positive spermatogonia are detected in both control and SMRT^{mRID} testes at 4 mo of age. (*J*) Seminiferous tubule histology after 7 mo of a Vitamin A-deficient diet (VAD). Complete block of spermatogonial differentiation is evident in WT control tubules while in SMRT^{mRID} tubules, ongoing spermatogenesis was evident. TRA98 staining was used to detect germ cell population. Arrowheads indicate differentiating spermatogonia. Weak TRA98 staining is detected in SMRT^{mRID} spermatocytes. (*K*) Testis and SV weights in mice maintained on a VAD diet (n = 6, $^{*}P < 0.01$). (Scale bar, 100 μm.)

transcribed prior to haploid germ cells entering spermiogenesis and the mRNAs stored in translationally inert ribonuclear particles (RNPs). We attribute the profound asynchrony in mutant testes, evidenced by the presence of steps 8 to 9 and steps 12 to 14 elongated spermatids in the same tubules, to different stages of spermatid differentiation rather than changes in the translational regulation of RNPs (*SI Appendix,* Fig. S3*A*). Interestingly, this asynchronous cell association is also seen in RARα null testes (22). As spermiation steps coincide with the highest concentration of RA in the tubules during spermatogenesis, similar phenotypic outcomes from the loss of RARα and the de-repression of RAR in SMRT^{mRID} appear contradictory. We posit that the loss of the RA-directed spermatogenic program, rather than simply the loss of RAR target gene regulation, contributes to this asynchrony in spermatogenesis.

Loss of Cyclical Gene Expression along the Seminiferous Tubules in SMRT^{mRID} Mice. Initiation of the spermatogenic cycle is spatially and temporally controlled along the length of seminiferous tubules. Cyclic spermatogenesis is thought to be regulated by cycles of steep RA gradients along the spermatogenic tubules (23–25). RA treatment after VAD-induced spermatogenic arrest resulted in synchronization of spermatogenic cycles, indicating RA is one of the components in these signaling gradients (11, 26). This action of RA can be visualized by its target gene expression in testicular cells (27). Sertoli cell-specific proteins GATA1 and androgen receptor (AR) are strongly expressed in stages VII–IX and VI–VII but not in III–IV and XI–XII, respectively. In SMRT^{mRID} testes, this stage-specific expression of GATA1 and AR was lost with both proteins expressed throughout the seminiferous cycles (Fig. 2*F*).

To determine the extent to which corepressor complexes affect RA-regulated pathways in testes, we examined the cyclic expression pattern of both germ cell and Sertoli cell-specific genes in prepubertal seminiferous tubules (Fig. 2*G*). In control testes, *Stra8*, which is normally expressed in spermatocytes and type A spermatogonia, displays a cyclic expression pattern in tubules at P7 (postnatal day 7). In SMRT^{mRID} tubules, this stage-dependent variation is lost with *Stra8* expression observed in all tubules, consistent with the de-repression of RAR target genes. Similarly, Sertoli cell-specific cyclic expression of *Stra6* and *Lgals1* (encoding galectin-1) were lost in SMRT^{mRID} tubules (Fig. 2*G*), phenocopying the cell-specific ablation of RARα in Sertoli cells (9, 27). In conjunction with the asynchronous cycle progression seen in the RARα KO mouse (22), our results strongly support the notion that repressor functions of SMRT are required to translate the

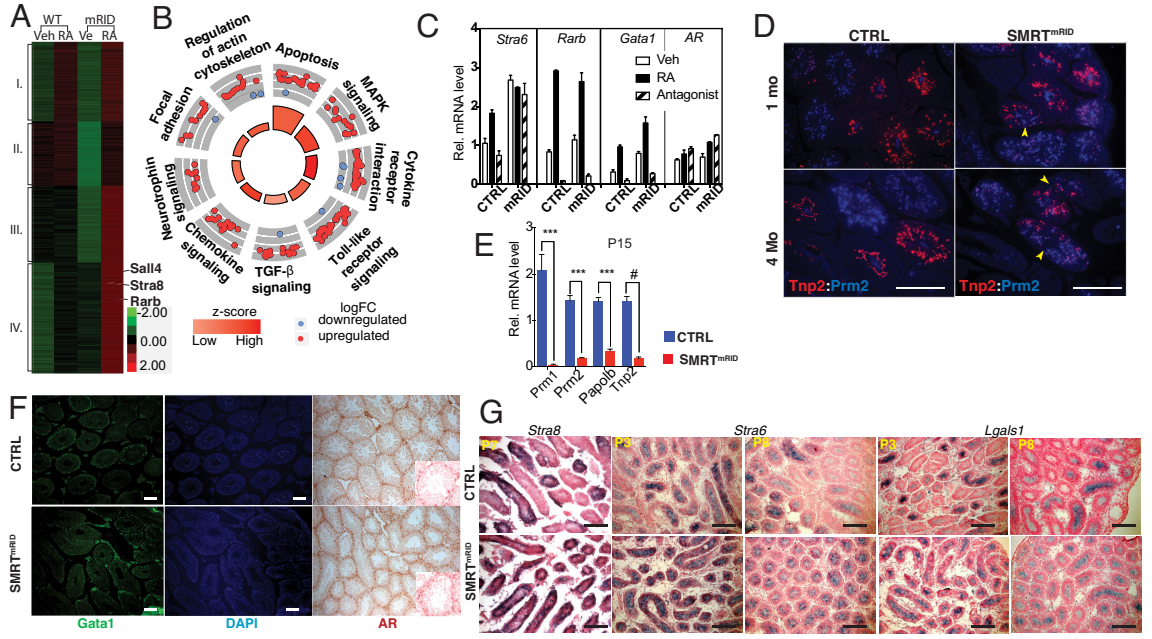

Fig. 2. De-repression of RAR target genes in Sertoli cells and asynchronous progression of spermatogenic cycle in SMRT^{mRID} mice. (*A*) Clustering of differentially expressed genes in control and SMRT^{mRID} GS cells in response to all trans RA. (*B*) KEGG pathway analysis of transcriptomes of Sertoli cells isolated from control and SMRT^{mRID} testes. Genome-wide transcriptome analysis of Sertoli cell-enriched fractions indicates the upregulation of several important pathways in SMRT^{mRID} Sertoli cells. (*C*) Relative transcript levels of RAR target genes *Stra6*, *RARb*, *Gata1*, and non-RAR target *AR* in CTRL and SMRT^{mRID} Sertoli cells in response to agonist (RA) and antagonist treatments. (*D*) Immunofluorescence microscopy of Tnp2 and Prm2 in CTRL and SMRT^{mRID} Sertoli cells. Arrowheads indicate tubules showing asynchronous replacement of histones. (*E*) Elongated spermatid specific gene expression in CTRL and SMRT^{mRID} at postnatal day 15 (P15) ($N = 5$, $^{***}P < 0.005$; $^{\#}P < 0.0001$). (*F*) Stage-dependent Gata1 and AR expression in CTRL and SMRT^{mRID} seminiferous tubules. (*G*) Prepubertal cyclical *Stra8*, *Stra6,* and *Lgals1* expression in CTRL and SMRT^{mRID} seminiferous tubules. Seminiferous cycle-dependent cyclical expression of *Stra8*, *Stra6,* and *Lgals1* (Galectin-1) is lost in SMRT^{mRID} tubules shown by in situ hybridization. (Scale bar, 100 μm.)

repeating pulses of RA along the seminiferous tubules into the cyclic expression of RAR targets (15, 28, 29). We posit that SMRT dissociation from RAR results in imprecise readouts of the RA pulses as clear ON/OFF signals, resulting in the disruption of cyclic expression of both germ and Sertoli cell-stage-specific targets, which ultimately disrupt the synchronized progression of the spermatogenic cycle along the tubule.

Compromised Spermatogenesis in SMRT^{mRID} Mice. While there was no evidence of increased apoptosis in the seminiferous tubules of SMRT^{mRID} mice, few mature sperm were present in the caudal epididymis. Rather, SMRT^{mRID} epididymides were filled with mostly apoptotic post-meiotic spermatids (Fig. 3*A* and *SI Appendix,* Fig. S3*C*). These findings implicate defective Sertoli cell-round spermatid interactions resulting in the premature release of round spermatids into the epididymis. In addition, the germ cell layer of spermatocytes with step 7 spermatid was absent in subsets of SMRT^{mRID} tubules (*SI Appendix,* Fig. S3*B*), replicating the phenotype associated with spermatogonia-specific deletion of RARα (30). These tubules would miss round spermatids during the next cycle because there are no spermatocytes available to produce new spermatids. As there are no or very few spermatogonia present in the indicated tubules they might well be Sertoli cell only from the next cycle onwards (*SI Appendix,* Fig. S3*B*). Notably, the coordinated appearance of epithelium stages is lost, consistent with the loss of stage-specific cyclical gene expression in SMRT^{mRID} testis.

In order to determine the ability of somatic cells in SMRT^{mRID} testis to support spermatogenesis, germ cells were depleted in control and SMRT^{mRID} testis prior to spermatogonial transplantation (Fig. 3*B* and *SI Appendix,* Fig. S3*D*). While transplanted spermatogonia did survive, they were unable to fully repopulate SMRT^{mRID} tubules, implicating additional defects in the supporting somatic cells. Indeed, the reduced expression levels of the primary RA synthetic enzymes *Aldh1a2* and *Aldh1a1* in SMRT^{mRID} Sertoli cells provide a mechanism for altered spermatogenic differentiation (*SI Appendix,* Fig. S3*E*) (25).

Depolarized Microtubules and Cytoskeletons in SMRT^{mRID} Tubules. While the prepubertal first round of spermatogenesis appears relatively normal in SMRT^{mRID} mice (*SI Appendix,* Fig. S3*F*), immunostaining of vimentin and tyrosinated tubulin revealed abnormalities in Sertoli nuclei and microtubule polarization in the seminiferous tubules, respectively (Fig. 3*C*). In control tubules, Sertoli nuclei are located near the basal lamina and oriented toward the lumen as visualized with vimentin filaments projected toward lumen. In SMRT^{mRID} tubules, this typical polarized vimentin projection of Sertoli nuclei is often lost and the polarized microtubule formation toward the lumen is disorientated. In addition, alterations in Sertoli-germ cell junctions were evidenced by espin staining of SMRT^{mRID} tubules (Fig. 3*D*). Alternatively, this observation could be due to the loss of germ cells with the preservation of Sertoli cell numbers and their cytoplasm in SMRT^{mRID} tubules. In general, Sertoli cells move toward the lumen in the tubules with a severe germ cell loss, eventually causing more Sertoli cell loss. However, despite the presence of dislodged Sertoli cells in the central lumen, the blood–testis barrier (BTB) was not compromised in SMRT^{mRID} tubules based on the intravenous injection of Evans blue dye (Fig. 3*E*).

Histone Deacetylase Inhibition Phenocopies SMRT^{mRID} De-repression. The transcriptional repressive activity of SMRT is mediated through the histone deacetylase (HDAC) components of the corepressor complex. HDACs reduce chromatin accessibility at gene regulatory regions by removing lysine acetylation on the N-terminal tails of core histones. In GS cell cultures from neonatal and adult SSCs, the pan-HDAC inhibitor Valproic acid relieved

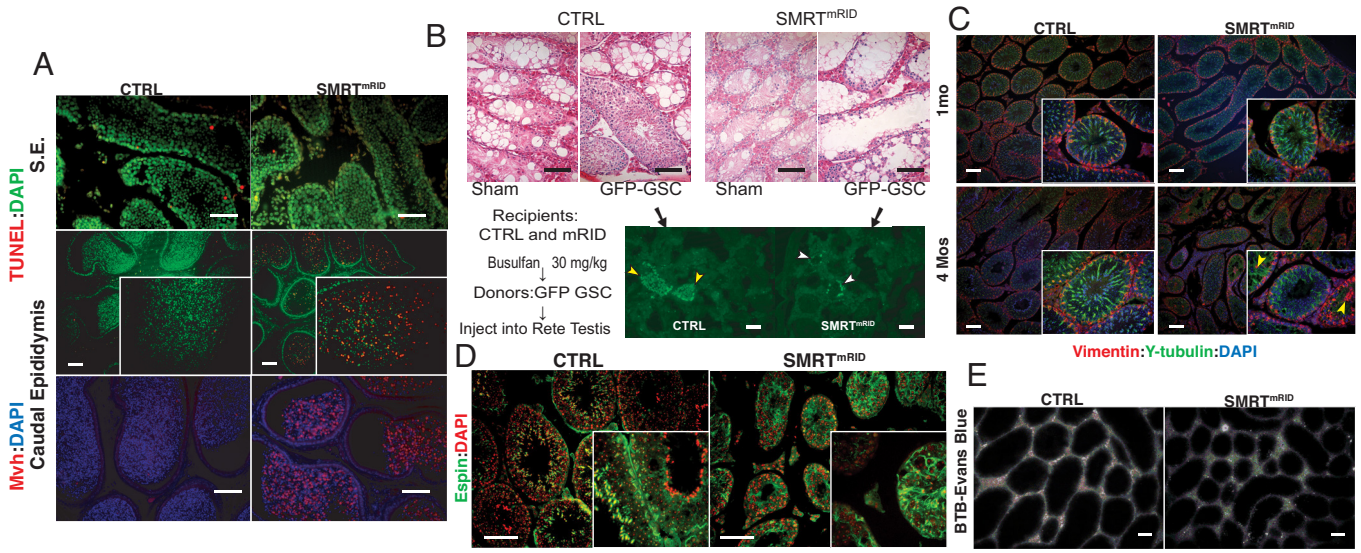

Fig. 3. Loss of differentiating germ cells and defective cytoskeleton network in SMRT^{mRID} Sertoli cells. (*A*) Apoptotic differentiating germ cells in epididymis but not in S.E. Apoptotic cells were detected by TUNEL assays and germ cells were detected by Mvh immunostaining. (*B*) Germ cell transplantation assay. GFP-positive germ stem cells (GSC) were transplanted into Busulfan-treated germ-cell-depleted WT control or SMRT^{mRID} recipient testes. Yellow arrowheads indicate repopulation of GFP-GSC in control recipients. White arrowheads indicate transplanted GFP-GSC without repopulation in SMRT^{mRID} environment. (*C*) Depolarized microtubule formation in SMRT^{mRID} tubules. Vimentins visualize Sertoli cell nuclei and project into the lumen in control but not in SMRT^{mRID}. Tyrosinated tubulins project into the center of the lumen while in SMRT^{mRID}, this projection is disorganized. Yellow arrowheads indicate detached Sertoli cells from basal lamina in SMRT^{mRID}. (*D*) Disorganized Sertoli–germ cell junction, ectoplasmic specialization in SMRT^{mRID} tubules. Espin antibody stains BTB and Sertoli–germ cell junction. (*E*) BTB is not compromised in SMRT^{mRID} testes (4 mo old). Permeability to intravenous injected Evans Blue dye to the S.E. was visualized by fluorescence microscopy. (Scale bar, 100 μm.)

repression of the RAR target gene, *Stra8*, to a similar extent as seen in SMRT^{mRID} cells (Fig. 4*A*). In addition, *Stra*8 was depressed by the Class I HDAC-selective inhibitor MS-275 in P19 embryonal carcinoma (EC) cells (Fig. 4*B*). These results indicate that pharmacologic inhibition of HDACs can phenocopy SMRT^{mRID}-mediated epigenetic changes to de-repress RAR target genes.

To assess the in vivo efficacy of HDAC inhibitors in disrupting mouse spermatogenesis, mice were treated with MS-275, an orally bioavailable inhibitor with FDA break-through status. The drug was well tolerated, with no loss of body weight in wild-type C57BL/6 male mice treated with increasing doses for 30 d (5, 10, and 20 mg/kg q.d.) (Fig. 4*D*). SV weight was not affected by drug treatment, indicating that there was no significant change in serum testosterone levels (*SI Appendix,* Fig. S4*A*). However, the testis size was dose-dependently reduced (Fig. 4*C*), and spermatogenesis was severely impacted, with few haploid germ cells in the tubules and virtually no sperm in the epididymis (Fig. 4*E* and *SI Appendix,* Figs. S4*B* and S5*A*). Remarkably, this disruption of spermatogenesis was reversible upon cessation of MS-275 treatment, suggesting that SSCs are not depleted during the drug treatment (Fig. 4*E* and *SI Appendix,* Fig. S5*A*). Indeed, PLZF+ SSCs were detected after MS-275 treatment (*SI Appendix,* Fig. S5*B*). MS-275-treated mice failed to sire offspring after 60 d of treatment, compared to litters of ~10 by the vehicle group (Fig. 4*F* and *SI Appendix,* Fig. S4*C*). However, fertility was restored 60 d after the cessation of MS-275 treatment. Importantly, no developmental defects were seen in pups produced by either F1 or F2 offspring. As a proof of principle, our findings indicate that chronic, oral administration of MS-275 transiently blocks male fertility without permanently affecting reproductive capacity or the genomic integrity of sperm.

Discussion

RARs play crucial roles in the regulation of spermatogenesis. As male germ cells differentiate from SSCs, the number of SSCs has to be maintained to balance the differentiation and self-maintenance of these cells. Even though there is a severe reduction of germ cells in SMRT^{mRID}, the presence of PLZF^{+} SSCs in SMRT^{mRID} mice indicates that the defects reside in aberrant differentiation of germ cells and interaction with Sertoli cells and not in SSC maintenance. We found varying stages of apoptotic primary spermatocytes to round spermatids in SMRT^{mRID} epididymides. RA signaling has been shown to regulate the release of spermatozoa from Sertoli cell cytoplasm during spermiation (14) and de-repression of RAR signaling could prematurely release differentiating germ cells from Sertoli cells. Alternatively, this loss of differentiating germ cells might be due to defects in the cytoskeletal network and specialized junctions in Sertoli cells. It is noteworthy to mention that the BTB is not compromised, despite the mis-localization of Sertoli cells in the seminiferous epithelium. As a complex network of tight, adherent and gap junctions facilitates the BTB, the selective disruption of germ cell-Sertoli cell interactions without impacting barrier function is possible.

The cyclical pattern of gene expression along the seminiferous tubules has been shown to correlate with pulses of RA peaking around stages VIII–IX of the seminiferous epithelium cycle (23, 31). The loss of this cyclical gene expression in SMRT^{mRID} mice resembles that observed in the Sertoli-specific RARα KO model. In SMRT^{mRID} mice, the disruption of RAR-mediated repression results in target gene activation at lower levels of RA and subsequently, the loss of spatial transcriptional regulation (Fig. 4 *G* and *H*).

Interestingly, in SMRT^{mRID} spermatogenesis, there is an asynchrony of differentiation in the tubule, as visualized by immunostaining of DNA wrapping proteins, transition proteins and protamines during histone replacement of round spermatids into elongated spermatids. In SMRT^{mRID} mice, elongating spermatids in different stages of differentiation were seen in single cross-sectional tubule planes with varying degree of histone replacements, some showing transition protein expression while some showed protamine expression, clearly indicating asynchronous spermiation process.

The most intriguing aspect of SMRT^{mRID} spermatogenesis is its resistance to Vitamin A deficiency. The fact that SMRT^{mRID}

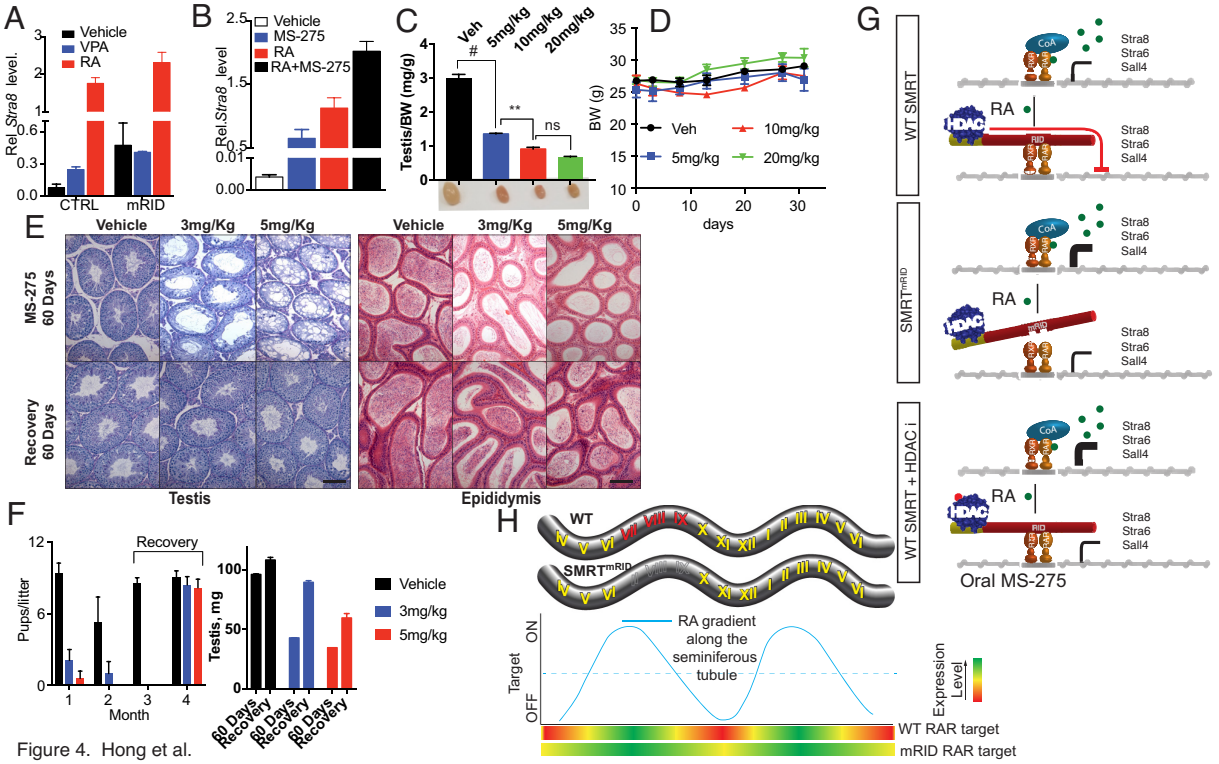

Figure 4. Hong et al.

Fig. 4. Histone deacetylase inhibition blocks mouse spermatogenesis. (*A*). RAR target gene, *Stra8* was de-repressed by HDAC inhibition in GS cells. (*B*) Class I HDAC inhibitor, MS-275 de-repressed *Stra8* in P19 EC cells. (*C*) 30-d-regimen of oral MS-275 dramatically shrank testis size. $N = 4$; ns, not significant; $^{**}P < 0.005$; $^{\#}P < 0.0001$. (*D*) The body weights of mice undergoing MS-275 regimens. (*E*) Testis and epididymis histology after 60 d MS-275 treatment and after recovery period. PAS stain for testis (*Left*) and H&E stain for caudal epididymis (*Right*). (*F*) The number of pups born per litter is shown during and after MS-275 treatment. $N = 5$ for 3 or 5 mg/kg regimens, $N = 3$ for vehicle control. (*G*) Model for SMRT^{mRID} derepression of RAR targets during spermatogenesis. (*H*) Loss of SMRT-mediated repression in RAR signaling downshifts target gene expression threshold, this leads to loss of gene expression gradients along the seminiferous tubules in SMRT^{mRID}. (Scale bar, 100 μm.)

SSCs still differentiate into spermatocytes without RA suggests that de-repressed RAR action in either SSCs or Sertoli could be responsible for the release of VAD-induced arrest of differentiation. It is also intriguing that SSCs are not depleted in aged SMRT^{mRID} mice in spite of an increased differentiation signal coming from de-repression of RAR signaling. It is conceivable that a subset of RA-resistant SSCs could be immune from de-repressed RAR signaling. Alternatively, as exogenous RA exposure does not change SSC numbers, SSCs could be replenished from Stra8^{+} spermatogonia (32).

The current studies in the unique knock-in corepressor mutant model identify RAR-dependent repression as a new regulatory component of spermatogenesis, especially in establishing cyclical gene expression patterns along the seminiferous tubules. This work also supports SMRT as the predominant RAR corepressor during spermatogenesis, as the closely related SMRT homolog NCoR is intact in this mouse model. At least in spermatogenesis, the preferential role of the SMRT corepressor might be due to its spatial expression pattern. SMRT expression is highest in SSC and Sertoli cells while NCoR expression is not cell-type specific. In our study, we also found that activation of RARs leads to induction of SMRT expression with no change in NCoR expression (18). There seems to be a feedback loop to keep the action of certain NRs in check by regulation of SMRT expression. The SMRT^{mRID} mouse model provides unique opportunities to explore repression-mediated regulation in male gametogenesis, complementing the established VAD and RAR null models.

The finding of an intact germ stem cell population, despite the absence of functional spermatogenesis, raises the possibility of reversible contraception. In proof-of-principle studies, we show de-repression of RAR target genes and signaling and reversible disruption of spermatogenesis with the oral HDAC inhibitor MS-275 (Fig. 4*E*). Similarly, the pan-histone deacetylase inhibitor, Trichostatin A, blocked maturation of round spermatids but paradoxically, triggered hypo-acetylation of histones in elongating spermatids (33). While pharmacological inhibition of RA production (such as WIN18,446) arrests germ stem cell differentiation with spermatogenesis resuming in response to RA, this approach failed due to inhibitor toxicity associated with alcohol dehydrogenases (2, 4). An Aldh1a2 specific inhibitor, CM-121, failed to effectively stop spermatogenesis, possibly due to redundancy in RA production (3, 6). Our finding that oral MS-275 effectively disrupts RAR-driven transcriptional gradients essential for spermatogenesis implicates MS-275 as a putative reversible male contraceptive without deadly alcohol interaction. Furthermore, given the long half-life of MS-275 in humans, a once-a-week contraceptive pill is a possibility (34).

Materials and Methods

Animals. SMRT^{mRID} knock-in mice were generated by standard homologous recombination using an inserted *neo* cassette for positive selection and a *tk* cassette for negative selection. Chimeric mice were generated by microinjection of two independently targeted ES clones into blastocysts. Two independent mouse mutant lines were established. SMRT^{mRID} mice were backcrossed for at least four generations to sv129. Mice were fed Labdiet 5002 containing 18 IU/g vitamin A. All animal experiments were approved by the Institute of Animal Care and Use Committee (IACUC) of the Salk Institute.

Apoptosis Assay. TUNEL (terminal dUTP nick-end labeling) assay was used to detect apoptotic cells in the frozen testis sections per the manufacturer's instruction (Roche).

Gene Expression Analysis. DNA-free total RNA was used to generate cDNA and analyzed by SYBR green-based quantitative PCR. *SI Appendix,* Table S1 lists all q-PCR primers used in the analysis.

RNA-Seq. DNA-free total RNA was prepared from biological duplicates and quality confirmed using the Agilent 2100 Bioanalyzer and RNA-Seq libraries prepared using the Illumina TruSeq Stranded RNA Sample Preparation Kit v2. Multiplexed libraries were validated using the Agilent BioAnalyzer, normalized, and pooled for sequencing. High-throughput sequencing was performed on the HiSeq 2500 platform (Illumina) with a 100-bp read length yielding a mean read depth of 6.61×10^6 per sample. Image analysis and base calling were performed using Illumina CASAVA-1.8.2. Short-read sequences were mapped to the GRCm38 reference sequence using the STAR aligner (35). Known splice junctions from Ensembl were supplied to the aligner and de novo junction discovery was also permitted. Differential gene expression, statistical testing, and Ensembl-based annotation were performed using Cuffdiff 2 (36). Transcript expression was calculated as gene-level relative abundance in fragments per kilobase of exon model per million mapped fragments and employed correction for transcript abundance bias (37).

Immunofluorescent and Immunohistochemistry. Testes were fixed with either Bouin's (immunohistochemistry) or Carnoy's fixative (immunofluorescence) for paraffin embedding. *SI Appendix,* Table S2 lists all the antibodies used in the analysis.

Germ Cell Transplantation. Recipient mice were intraperitoneally injected with busulfan (40 mg/kg) in DMSO to deplete the germ cell population. Donor GFP-spermatogonial cells were enriched by fractionation method and injected into Busulfan-treated testis via rete testis using micro-glass needle.

Vitamin A Deficiency. Mice were maintained on Harlan Teklad TD.86143 diet for at least 7 mo after Postnatal day 10 to accomplish complete Vitamin A deficiency.

Retinoid Analysis. Retinoid levels were quantified using external calibration curves, and retinyl ester recovery was measured using retinyl acetate as an internal standard (38). See *SI Appendix* for detailed methods.

Germ Stem Cell Culture. This method was modified from previously reported mouse germline stem cell culture (39) and detailed steps are listed in *SI Appendix*.

Additional Methods. See *SI Appendix*.

Data, Materials, and Software Availability. Raw sequence read data can be obtained from NCBI BioProject PRJNA1045605 (40) and BioSamples SAMN38472291 (41), SAMN38472292 (42), SAMN38472293 (43), and SAMN38472294 (44). All other data are included in the manuscript and/or *SI Appendix*.

ACKNOWLEDGMENTS. We thank Yang Dai and Yunqiang Yin for the technical support, Dr. Kistler, Stephen, Dr. Sungtae Kim and Dr. Hye-Won Song for reagents, E. Ong and C. Brondos for administrative support, and all Evans lab members for discussion. R.M.E. holds the March of Dimes Chair in Molecular and Developmental Biology at the Salk Institute and is a Nomis Distinguished Scholar. Research reported in this publication was supported by NIH Grant Nos. CA265762 and CA220468. The content is solely the responsibility of the authors and does not necessarily represent the official views of the NIH. This study was supported by the NGS and Flow Cytometry Salk Cores, which are funded by the Salk Cancer Center (NCI Grant: NIH-NCI CCSG: P30 014195).

1. M. Y. Roth, J. K. Amory, Beyond the condom: Frontiers in male contraception. *Semin. Reprod. Med.* **34**, 183–190 (2016).
2. J. K. Amory *et al.*, Suppression of spermatogenesis by bisdichloroacetyldiamines is mediated by inhibition of testicular retinoic acid biosynthesis. *J. Androl.* **32**, 111–119 (2011).
3. Y. Chen *et al.*, Structural basis of ALDH1A2 inhibition by irreversible and reversible small molecule inhibitors. *ACS Chem. Biol.* **13**, 582–590 (2018).
4. J. Paik *et al.*, Inhibition of retinoic acid biosynthesis by the bisdichloroacetyldiamine WIN 18,446 markedly suppresses spermatogenesis and alters retinoid metabolism in mice. *J. Biol. Chem.* **289**, 15104–15117 (2014).
5. M. A. A. Noman, J. L. Kyzer, S. S. W. Chung, D. J. Wolgemuth, G. I. Georg, Retinoic acid receptor antagonists for male contraception: current statusdagger. *Biol. Reprod.* **103**, 390–399 (2020).
6. E. Anthes, Why we can't have the male pill. Blloomberg. https://www.bloomberg.com/news/features/2017-08-03/why-we-can-t-have-the-male-pill. Accessed 17 January 2019.
7. S. S. Chung, X. Wang, D. J. Wolgemuth, Prolonged oral administration of a pan-retinoic acid receptor antagonist inhibits spermatogenesis in mice with a rapid recovery and changes in the expression of influx and efflux transporters. *Endocrinology* **157**, 1601–1612 (2016).
8. M. Teletin, N. Vernet, N. B. Ghyselinck, M. Mark, Roles of retinoic acid in germ cell differentiation. *Curr. Top Dev. Biol.* **125**, 191–225 (2017).
9. A. Gely-Pernot *et al.*, Retinoic acid receptors control spermatogonia cell-fate and induce expression of the SALL4A transcription factor. *PLoS Genet.* **11**, e1005501 (2015).
10. M. D. Griswold, Spermatogenesis: The commitment to meiosis. *Physiol. Rev.* **96**, 1–17 (2016).
11. A. M. van Pelt, D. G. de Rooij, Retinoic acid is able to reinitiate spermatogenesis in vitamin A-deficient rats and high replicate doses support the full development of spermatogenic cells. *Endocrinology* **128**, 697–704 (1991).
12. E. K. Velte *et al.*, Differential RA responsiveness directs formation of functionally distinct spermatogonial populations at the initiation of spermatogenesis in the mouse. *Development* **146**, dev173088 (2019).
13. J. T. Busada, C. B. Geyer, The role of retinoic acid (RA) in spermatogonial differentiation. *Biol. Reprod.* **94**, 10 (2016).
14. M. Mark, M. Teletin, N. Vernet, N. B. Ghyselinck, Role of retinoic acid receptor (RAR) signaling in post-natal male germ cell differentiation. *Biochim. Biophys. Acta* **1849**, 84–93 (2015).
15. C. A. Hogarth *et al.*, CYP26 enzymes are necessary within the postnatal seminiferous epithelium for normal murine spermatogenesis. *Biol. Reprod.* **93**, 19 (2015).
16. R. R. Nofsinger *et al.*, SMRT repression of nuclear receptors controls the adipogenic set point and metabolic homeostasis. *Proc. Natl. Acad. Sci. U.S.A.* **105**, 20021–20026 (2008).
17. S. H. Hong *et al.*, Rescue of a primary myelofibrosis model by retinoid-antagonist therapy. *Proc. Natl. Acad. Sci. U.S.A.* **110**, 18820–18825 (2013).
18. S. H. Hong *et al.*, Corepressor SMRT is required to maintain Hox transcriptional memory during somitogenesis. *Proc. Natl. Acad. Sci. U.S.A.* **115**, 10381–10386 (2018).
19. A. M. van Pelt *et al.*, Characteristics of A spermatogonia and preleptotene spermatocytes in the vitamin A-deficient rat testis. *Biol. Reprod.* **53**, 570–578 (1995).
20. P. J. Alfonso, W. S. Kistler, Immunohistochemical localization of spermatid nuclear transition protein 2 in the testes of rats and mice. *Biol. Reprod.* **48**, 522–529 (1993).
21. M. A. Heidaran, R. M. Showman, W. S. Kistler, A cytochemical study of the transcriptional and translational regulation of nuclear transition protein 1 (TP1), a major chromosomal protein of mammalian spermatids. *J. Cell Biol.* **106**, 1427–1433 (1988).
22. S. W. C. Sanny, S. Wengkong, W. Xiangyuan, J. W. Debra, Retinoic acid receptor alpha is required for synchronization of spermatogenic cycles and its absence results in progressive breakdown of the spermatogenic process. *Dev. Dyn.* **230**, 754–766 (2004).
23. T. Endo, E. Freinkman, D. G. de Rooij, D. C. Page, Periodic production of retinoic acid by meiotic and somatic cells coordinates four transitions in mouse spermatogenesis. *Proc. Natl. Acad. Sci. U.S.A.* **114**, E10132–E10141 (2017).
24. T. Endo *et al.*, Periodic retinoic acid-STRA8 signaling intersects with periodic germ-cell competencies to regulate spermatogenesis. *Proc. Natl. Acad. Sci. U.S.A.* **112**, E2347–E2356 (2015).
25. M. Raverdeau *et al.*, Retinoic acid induces Sertoli cell paracrine signals for spermatogonia differentiation but cell autonomously drives spermatocyte meiosis. *Proc. Natl. Acad. Sci. U.S.A.* **109**, 16582–16587 (2012).
26. A. M. van Pelt, D. G. de Rooij, Synchronization of the seminiferous epithelium after vitamin A replacement in vitamin A-deficient mice. *Biol. Reprod.* **43**, 363–367 (1990).
27. N. Vernet *et al.*, Prepubertal testis development relies on retinoic acid but not rexinoid receptors in Sertoli cells. *EMBO J.* **25**, 5816–5825 (2006).
28. N. Vernet *et al.*, Retinoic acid metabolism and signaling pathways in the adult and developing mouse testis. *Endocrinology* **147**, 96–110 (2006).
29. J. W. Wu, R. Y. Wang, Q. S. Guo, C. Xu, Expression of the retinoic acid-metabolizing enzymes RALDH2 and CYP26b1 during mouse postnatal testis development. *Asian J. Androl.* **10**, 569–576 (2008).
30. A. Gely-Pernot *et al.*, Spermatogonia differentiation requires retinoic acid receptor gamma. *Endocrinology* **153**, 438–449 (2012).
31. C. A. Hogarth *et al.*, Processive pulses of retinoic acid propel asynchronous and continuous murine sperm production. *Biol. Reprod.* **92**, 37 (2015).
32. K. S. Agrimson *et al.*, Retinoic acid deficiency leads to an increase in spermatogonial stem number in the neonatal mouse testis, but excess retinoic acid results in no change. *Dev. Biol.* **432**, 229–236 (2017).
33. I. Fenic, V. Sonnack, K. Failing, M. Bergmann, K. Steger, In vivo effects of histone-deacetylase inhibitor trichostatin-A on murine spermatogenesis. *J. Androl.* **25**, 811–818 (2004).
34. R. M. Connolly, M. A. Rudek, R. Piekarz, Entinostat: A promising treatment option for patients with advanced breast cancer. *Future Oncol.* **13**, 1137–1148 (2017).
35. A. Dobin *et al.*, STAR: Ultrafast universal RNA-seq aligner. *Bioinformatics* **29**, 15–21 (2013).
36. C. Trapnell *et al.*, Differential analysis of gene regulation at transcript resolution with RNA-seq. *Nat. Biotechnol.* **31**, 46–53 (2013).
37. A. Roberts, C. Trapnell, J. Donaghey, J. L. Rinn, L. Pachter, Improving RNA-Seq expression estimates by correcting for fragment bias. *Genome Biol.* **12**, R22 (2011).
38. M. A. Kane, A. E. Folias, C. Wang, J. L. Napoli, Quantitative profiling of endogenous retinoic acid in vivo and in vitro by tandem mass spectrometry. *Anal. Chem.* **80**, 1702–1708 (2008).
39. M. Kanatsu-Shinohara *et al.*, Long-term culture of mouse male germline stem cells under serum-or feeder-free conditions. *Biol. Reprod.* **72**, 985–991 (2005).
40. R. Yu, The Salk Institute for Biological Studies, Targeting nuclear receptor corepressors for reversible male contraception. NCBI Bioproject. https://www.ncbi.nlm.nih.gov/bioproject/1045605. Deposited 27 November 2023.
41. R. Yu, The Salk Institute for Biological Studies, CTRL_sertoli_1_Stranded. NCBI Biosample. https://www.ncbi.nlm.nih.gov/biosample/38472291. Deposited 28 November 2023.
42. R. Yu, The Salk Institute for Biological Studies, CTRL_sertoli_2_Stranded. NCBI Biosample. https://www.ncbi.nlm.nih.gov/biosample/38472292. Deposited 28 November 2023.
43. R. Yu, The Salk Institute for Biological Studies, mRID_sertoli_1_Stranded. NCBI Biosample. https://www.ncbi.nlm.nih.gov/biosample/38472293. Deposited 28 November 2023.
44. R. Yu, The Salk Institute for Biological Studies, mRID_sertoli_2_Stranded. NCBI Biosample. https://www.ncbi.nlm.nih.gov/biosample/38472294. Deposited 28 November 2023.